Structure, Vol. 10, 413–424, March, 2002, ©2002 Elsevier Science Ltd. All rights reserved. PII S0969-2126(02)00725-6

Structural Milestones in the Reaction Pathway of an Amide Hydrolase: Substrate, Acyl, and Product Complexes of Cephalothin with AmpC β-Lactamase

Beth M. Beadle, Indi Trehan, Pamela J. Focia, and Brian K. Shoichet[1]
Department of Molecular Pharmacology and Biological Chemistry
Northwestern University
303 East Chicago Avenue
Mail Code S215
Chicago, Illinois 60611

Summary

β-lactamases hydrolyze β-lactam antibiotics and are the leading cause of bacterial resistance to these drugs. Although β-lactamases have been extensively studied, structures of the substrate-enzyme and product-enzyme complexes have proven elusive. Here, the structure of a mutant AmpC in complex with the β-lactam cephalothin in its substrate and product forms was determined by X-ray crystallography to 1.53 Å resolution. The acyl-enzyme intermediate between AmpC and cephalothin was determined to 2.06 Å resolution. The ligand undergoes a dramatic conformational change as the reaction progresses, with the characteristic six-membered dihydrothiazine ring of cephalothin rotating by 109°. These structures correspond to all three intermediates along the reaction path and provide insight into substrate recognition, catalysis, and product expulsion.

Introduction

The expression of β-lactamases is the most common cause of resistance to the β-lactam class of antibiotics [1, 2]. The mechanism of action of these enzymes is of great interest because of their threat to public health. Of the four classes of β-lactamases, class A, C, and D enzymes use a catalytic serine to hydrolyze the β-lactam ring, and class B enzymes use metal cofactors [3]. Class C β-lactamases, such as AmpC, are a growing concern because of their prevalence in Gram-negative hospital-acquired pathogens.

Class C β-lactamases hydrolyze the β-lactam bond of these antibiotics in a four-step process involving the formation of three intermediates (Figure 1). Like serine proteases, serine β-lactamases first form a precovalent encounter complex with their substrates (intermediate 1). This complex positions the substrate for nucleophilic attack by an activated serine, Ser64 in class C enzymes, which results in the formation of a relatively stable covalent acyl-enzyme (intermediate 2). This acyl-enzyme is then attacked by water, which breaks the covalent acyl-enzyme bond, and results in a noncovalent product-enzyme complex (intermediate 3) and subsequently free enzyme.

Class C β-lactamases have been intensely studied both mechanistically and structurally. Early mutagenesis [4–8] and structural [9–11] work identified key catalytic residues. Subsequent X-ray crystallographic work has investigated acyl-adduct complexes of the enzymes with β-lactam inhibitors and poor substrates, such as aztreonam [9], moxalactam [12], ceftazidime [13], and a cephem sulfone [14]. Complexes of the enzyme with β-lactam substrates, like loracarbef [12], have been captured through the use of deacylation-deficient mutant enzymes. These complexes revealed key interactions that contribute to β-lactam binding in the acyl state. In addition, covalent adducts with transition-state analogs have suggested the identity of the hydrolytic water and offered a structural view of how the enzyme stabilizes the deacylation transition state [15–17].

Despite this wealth of structural information, all previous complexes have captured the β-lactamase interacting with a β-lactam or transition-state analog in an acyl state; therefore, little is known about how the substrate is first recognized. This precovalent, first encounter complex is highly transient; the strain of the four-membered β-lactam ring and the nucleophilicity of Ser64 makes covalent bond formation very rapid. Thus, the precovalent substrate-enzyme complex has not been observed structurally. Similarly, the hydrolyzed product of the reaction has never been observed in the active site of a β-lactamase. This is consistent with enzymatic studies that have failed to show any appreciable product inhibition [18, 19]. Serine β-lactamases have been described as "perfect" enzymes [20, 21], and part of their proficiency arises from being able to distinguish between substrates and products. The basis for precovalent substrate recognition and selectivity over product binding remains unknown.

Efforts to capture crystal structures of precovalent enzyme-substrate and postcovalent enzyme-product complexes have been undertaken in other enzymes and, although technically challenging, have proven to be mechanistically illuminating [22–27]. Recently, the noncovalent Michaelis complex of a tetrapeptide substrate has been captured with an inactivated form of D-Ala-D-Ala-peptidase R61; the product complex with the active form of the enzyme has also been observed [26]. Complexes of Factor XIII activation peptide, a substrate analog, with α-thrombin [25], fibrinogen-Aα, another substrate analog, with bovine thrombin [24], α-chymotrypsin with noncovalent product oligopeptides [22], and HIV-1 and SIV proteases with hydrolysis products [23] have also been observed through X-ray crystallography. The rare structures of these complexes have provided insight into both binding and catalysis. These complexes also demonstrated the limitations of analogs and acyl-intermediates in understanding recognition at other steps in the reaction pathway of these enzymes.

Here we report the X-ray crystal structures of the three intermediates in the reaction pathway of hydrolysis of the characteristic substrate cephalothin, a cephalospo-

[1]Correspondence: b-shoichet@northwestern.edu

Key words: AmpC; β-lactamase; cephalothin; substrate-enzyme complex; product-enzyme complex; X-ray crystallography

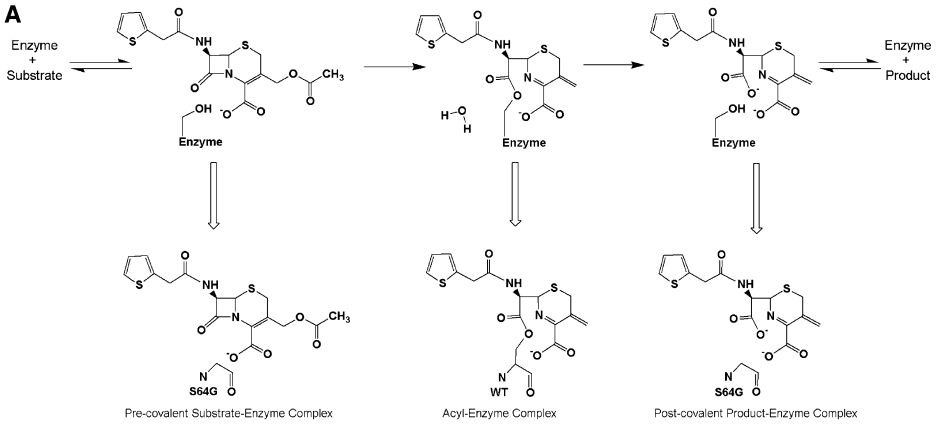

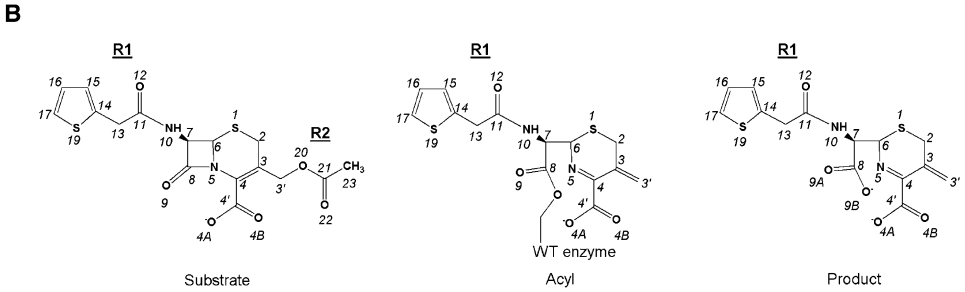

Figure 1. The Basic Reaction Pathway of a Serine β-Lactamase

(A) The pathway is shown with the stable intermediates (above) and the corresponding complexes that have been determined to understand each step (below). The substrate first binds to the enzyme to form a precovalent first encounter complex (left). Following nucleophilic attack by the catalytic serine, the enzyme and β-lactam are covalently bound in an acyl-enzyme complex (middle). Water then attacks the carbonyl carbon of the acyl-intermediate, hydrolyzing the covalent enzyme-ligand bond and generating the hydrolyzed product and intact enzyme (right). Finally, the product leaves, and the active enzyme is regenerated.

(B) Structural diagrams of substrate, acyl, and product forms of cephalothin. Interaction distances describing the interactions of substrate and product cephalothin with AmpC S64G and acyl cephalothin with AmpC WT are given in Table 2.

rin β-lactam, by AmpC β-lactamase (Figure 1). The mutant AmpC S64G was used to capture both the substrate and product of the reaction within the active site, and the structure of these complexes was determined to 1.53 Å resolution. In addition, an acyl complex of the wild-type (WT) enzyme with cephalothin was also captured; the structure of this complex was determined to 2.06 Å resolution. For the first time, the recognition of a good substrate by a β-lactamase can be observed as it undergoes acylation and then deacylation. The ligand itself undergoes dramatic conformational changes in the course of this hydrolysis; these changes help to explain substrate recognition, catalysis, and discharge of the product.

Results

S64G/Cephalothin Complex

The X-ray crystal structure of AmpC S64G in complex with cephalothin was determined to 1.53 Å resolution (Table 1; Figures 2A and 2C). Well-defined features in the initial $F_o - F_c$ electron density, contoured at 3 σ, revealed the presence of a ligand in each of the two active sites of the crystallographic asymmetric unit. Two different forms of cephalothin were observed; the precovalent substrate cephalothin, with its intact four-membered β-lactam ring, was bound in monomer 1, and the product of the reaction, hydrolyzed cephalothin, was bound in monomer 2. Refinement resulted in a model with a final R factor of 19.5% and a final R_{free} of 22.0% using data from 20 to 1.53 Å. Simulated-annealing omit maps of the active site ligands in the final model confirmed their identities and conformations (Figures 2A and 2C). The stereochemistry of the model was evaluated by the program Procheck [28]; 92.3% of the nonproline, nonglycine residues were in the most favored region of the Ramachandran plot, and 7.7% were in the additionally allowed region. As compared to a WT AmpC structure determined to 1.72 Å (Protein Data Bank entry 1KE4), the root-mean-square deviation (rmsd) of Cα positions between WT apo monomer 1 and S64G/cephalothin monomer 1 is 0.27 Å and WT apo monomer 2 and S64G/cephalothin monomer 2 is 0.15 Å.

Substrate-Enzyme Complex

Within the precovalent substrate-enzyme complex observed in monomer 1, there is no electron density between residue 64 and the bound substrate. It is also

Table 1. Data Collection and Refinement Statistics

	S64G/Cephalothin	WT/Cephalothin
Space group	C2	C2
Cell constants (Å)	a = 118.62, b = 77.15, c = 98.07; β = 115.90°	a = 117.69, b = 77.20, c = 97.59; β = 116.13°
Resolution (Å)	1.53	2.06
Number of molecules per asymmetric unit	2	2
Total reflections	385,475	168,893
Unique reflections	108,082	46,729
R_{merge} (%)[a]	6.6 (40.0)	6.2 (32.0)
Completeness (%)	90.3 (95.5)[b]	96.2 (83.4)
$<I>/<\sigma_I>$	28.2 (2.14)	23.2 (2.93)
Resolution range for refinement (Å)	20–1.53 (1.57–1.53)	20–2.06 (2.11–2.06)
Number of protein residues	716	712
Number of protein atoms in final model	5544	5541
Number of nonhydrogen ligand atoms (monomer 1 only)	26	NP[c]
Number of nonhydrogen ligand atoms (monomer 2 only)	23	22
Number of water molecules	488	339
Rmsd bond lengths (Å)	0.014	0.012
Rmsd bond angles (°)	1.7	1.7
R factor (%)	19.5	17.6
R_{free} (%)[d]	22.0	21.9
Average B factor, protein atoms (Å^2)	27.0	31.7
Average B factor, protein atoms (Å^2; monomer 1 only)	26.4	30.9
Average B factor, protein atoms (Å^2; monomer 2 only)	27.7	32.5
Average B factor, ligand atoms (Å^2; monomer 1 only)	49.3[e]	NP
Average B factor, ligand atoms (Å^2; monomer 2 only)	42.5[f]	50.5
Average B factor, solvent (Å^2)	35.1	37.3

[a] Values in parentheses are for the highest resolution shell used in refinement.
[b] The higher completeness of the last resolution bin reflects the presence of ice rings in a few of the lower resolution bins. Reflections in these ice rings were rejected, thereby lowering the overall completeness.
[c] NP, not present. For WT/cephalothin, the ligand was modeled only in monomer 2 as the acyl cephalothin; it is modeled at an occupancy of 0.8. For monomer 1, no ligand was observed.
[d] R_{free} was calculated with 2.5% and 5.0% of reflections set aside randomly for S64G and WT, respectively.
[e] For S64G/cephalothin, the ligand in monomer 1 is the substrate cephalothin; it is modelled at an occupancy of 0.65.
[f] For S64G/cephalothin, the ligand in monomer 2 is the product cephalothin; it is modelled at an occupancy of 0.9.

clear that the occupancy of the substrate is less than 1.0; tetrahedral density overlaps the proximal portion of the β-lactam ring, suggesting a bound phosphate, which corresponds to one observed in the AmpC S64G native structure (unpublished data). The occupancy of the substrate was set to 0.65, and that of the phosphate was set to 0.35.

In the precovalent substrate complex with S64G, the O9 carbonyl oxygen of the β-lactam ring is recognized in the "electrophilic" [11] or "oxyanion" [29] hole by the main chain nitrogens of Gly64 (2.8 Å) and Ala318 (2.8 Å) and makes a close contact with the main chain oxygen of Ala318 (3.1 Å) (Table 2; Figure 3A). The six-membered dihydrothiazine ring of cephalothin is locked into position since it remains fused to the intact four-membered β-lactam ring. The characteristic C4′ carboxylate is directed "down" toward the bottom of the active site; the O4A oxygen appears to accept a hydrogen bond from the putative catalytic base, Tyr150 (3.2 Å) and Thr316 (3.2 Å), and the O4B oxygen hydrogen bonds with Wat401, a well-ordered water molecule that is seen in many structures [12–14, 16] and corresponds to Wat403 in monomer 2. Wat401 also interacts with Asn346 and Arg349. There is no water in the active site that corresponds to the deacylating water (Wat400 in monomer 1, and Wat402 in monomer 2 of other structures); instead, this site is occupied by the C4′ carboxylate of the ligand. The R2 leaving group of the substrate makes few interactions in the active site (Figure 3A), pointing toward bulk solvent in an area of relative disorder in the structure (residues 280 to 295). On the other side of the molecule, the amide group of the R1 side chain is recognized by Gln120, Asn152, and the main chain oxygen of Ala318, as expected [9, 12, 15] (Table 2). The more distal portion of the R1 side chain, the thiophene ring of cephalothin, π stacks with Tyr221; the centroids of these two rings are 4.4 Å away from each other, and their planes are at an angle of 21°.

Product-Enzyme Complex

In monomer 2 of the S64G/cephalothin complex, simulated-annealing omit electron density reveals that the bound ligand is the hydrolyzed, postcovalent form of cephalothin, the product of the reaction (Figure 2C); it

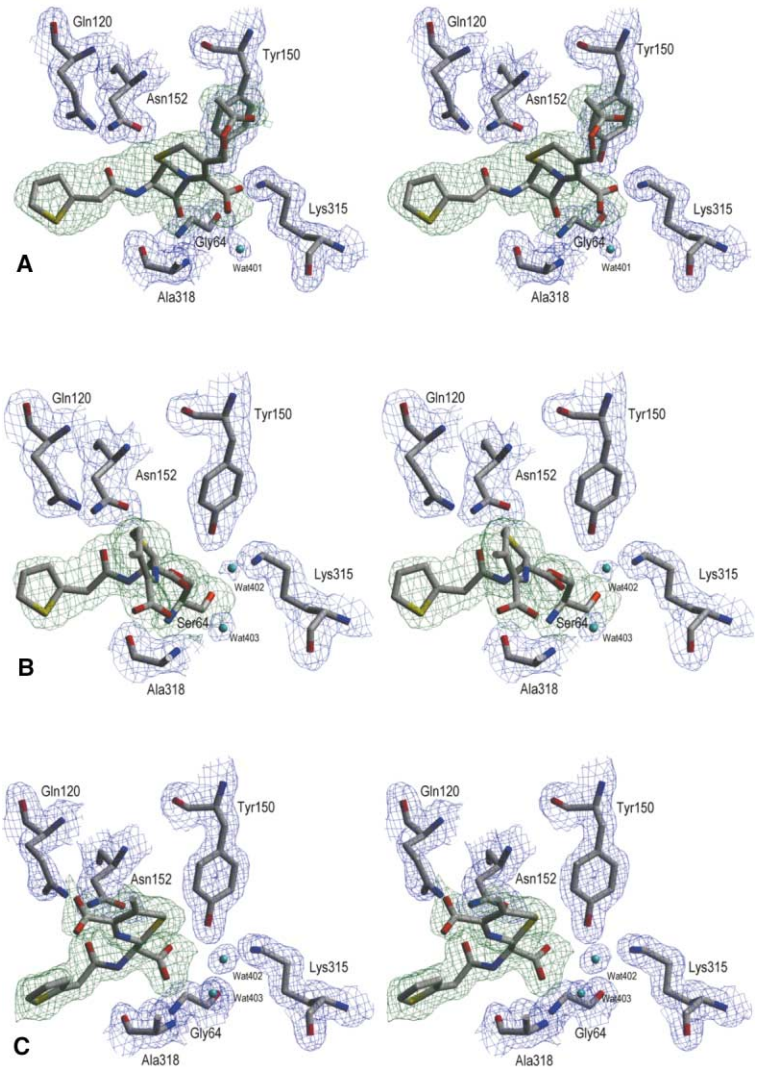

Figure 2. Stereoviews of the Active Site Electron Density for Each Complexed Structure

For each, the $2F_o - F_c$ electron density of the refined model of AmpC is shown in blue, contoured at 1.0 σ, and the simulated-annealing omit electron density of the refined ligand is shown in green, contoured at 3.0 σ for the substrate (A) and 3.3 σ for both the acyl (B) and product (C) complexes. The active site region from monomer 1 of the asymmetric unit is shown for the substrate (A) complex, and the active site from monomer 2 of the asymmetric unit is shown for the acyl (B) and product (C) complexes. Carbon atoms, gray; oxygen atoms, red; nitrogen atoms, blue. Water molecules are indicated by cyan spheres. The figure was generated using SETOR [52].

was modeled at an occupancy of 0.9. Although we did not explicitly add product in the crystal-soaking experiment, the mutant S64G retains enough activity (72,000-fold down from WT; unpublished data) to produce a substantial amount of product over the time course of the experiment. With its four-membered ring broken and the R2 leaving group having departed, the product-enzyme complex shows a different set of interactions (Table 2; Figure 3C). The hydrolysis of the β-lactam ring results in a carboxylate, with oxygens O9A and O9B in place of the original carbonyl oxygen O9 of the substrate. The O9A oxygen of the newly formed carboxylate binds similarly to the O9 carbonyl oxygen of the substrate, hydrogen bonding to the main chain nitrogens of Gly64 (2.8 Å) and Ala318 (2.9 Å), but moves away from the main chain oxygen of Ala318. The other carboxylate oxygen, O9B, interacts with Lys67 (2.9 Å) and Tyr150 (2.6 Å). Without the four-membered ring to lock it in place, the six-membered dihydrothiazine ring rotates about the C6-C7 bond [30] so that its carboxylate is 109° from its original position in the substrate (as measured as the angle from C4′ [substrate] to C6 to C4′ [product]); the C4′ carbon of this carboxylate is 7.3 Å from its original position in the substrate complex (Figure 4A). The carboxylate loses its interactions with Tyr150 and Thr316, which were seen in the substrate structure, and now interacts with Gln120. The movement of the carboxylate opens up this area of the active site of monomer 2, and well-ordered waters Wat402 and Wat403 are observed. Wat402 is highly conserved in AmpC structures and is believed to be the deacylating water molecule [12, 14, 16]. On the other side of the molecule, the amide group of the R1 side chain is recognized by Gln120, Asn152, and the main chain oxygen of Ala318, as in the substrate. However, the thiophene ring has rotated such that it no longer can π stack with Tyr221. The centroids of the thiophene ring and Tyr221 have been displaced so that they are 5.8 Å away from each other, and their planes are at an angle of 86°. The change in the thiophene position may be due to the proximity of the C4′ carboxylate, which has rotated "up" to hydrogen bond with Gln120.

WT/Cephalothin Acyl-Enzyme Complex

The X-ray crystal structure of cephalothin in complex with the WT AmpC was determined to 2.06 Å resolution

Table 2. Key Interactions within the AmpC/Cephalothin Complexes

Interaction	Distance (Å)			
	S64G/substrate[a]	WT/acyl[b]	S64G/product[b]	Native AmpC[b,c]
Y150OH-K315Nζ	2.7	2.8	2.8	2.8
Y150OH-S64Oγ	NP[d]	3.1	NP	2.9
Y150OH-K67Nζ	2.9	3.1	2.9	3.3
K67Nζ-A220O	2.9	3.0	3.0	2.9
K67Nζ-S64Oγ	NP	3.2	NP	2.8
N152Oδ1-K67Nζ	2.7	2.7	2.7	2.6
N152Nδ2-Q120Oε1	3.0	2.9	2.8	2.8
S/G64N-O9	2.8	4.0	NP	NP
A318N-O9	2.8	3.4	NP	NP
A318O-O9	3.1	4.1	NP	NP
A318O-N10	3.1	3.0	2.9	NP
K67Nζ-O9B	NP	NP	2.9	NP
Y150OH-O9B	NP	NP	2.6	NP
G64N-O9A	NP	NP	2.8	NP
A318N-O9A	NP	NP	2.9	NP
N152Nδ2-O12	2.8	2.6	2.9	NP
Q120Nε2-O12	3.1	3.1	3.1	NP
Wat402-N5	NP	4.9	6.0	NP
Wat402-T316Oγ1	NP	3.1	2.7	3.0
Wat402-Wat403	NP	3.9	2.8	2.9
Wat402-O4B	NP	8.0	8.9	NP
Wat402-O9	NP	2.6	NP	NP
Wat402-Y150OH	NP	3.4	4.4	4.3
Wat403-N346Oδ1	NP	2.6	2.9	2.6
Wat403-R349Nη1	NP	2.9	3.1	2.9
Wat403-O4A	NP	3.7	8.2	NP
Wat401-O4B	2.4	NP	NP	NP
Wat401-N346Oδ1	2.6	NP	NP	NP
Wat401-R349Nη1	2.9	NP	NP	NP
Wat681-O22	2.5	NP	NP	NP
Y150OH-O4A	3.2	8.8	10.0	NP
T316Oγ1-O4A	3.2	7.6	11.4	NP
N343Nδ2-O4B	6.8	3.0	7.9	NP
Q120Nε2-O4B	9.0	7.6	2.9	NP

Structural diagrams are given in Figure 1B.
[a] Distances are for monomer 1 of the asymmetric unit.
[b] Distances are for monomer 2 of the asymmetric unit.
[c] From R.A. Powers and B.K.S. (unpublished data; Protein Data Bank entry 1KE4).
[d] NP, not present.

(Table 1; Figure 2B). Unambiguous $F_o - F_c$ electron density in the initial maps, contoured at 3 σ, revealed the presence of a ligand covalently linked to the Oγ of Ser64 in monomer 2 (Figure 2B); little difference density was seen in monomer 1. Cephalothin was modeled into the difference density of monomer 2 as its covalently bound, open ring form at an occupancy of 0.8. As expected, the R2 leaving group has departed, leaving an exocyclic methylene (C3′) off of the dihydrothiazine ring. A simulated-annealing omit map of the ligand in the final model confirmed the identity and conformation of the ligand (Figure 2B). The final R factor was 17.6%, and the final R_{free} was 21.9%. The stereochemistry of the model was evaluated by the program Procheck [28]; 91.6% of the nonproline, nonglycine residues were in the most favored region of the Ramachandran plot, and 8.4% were in the additionally allowed region. As compared to monomer 2 of the WT AmpC structure (Protein Data Bank entry 1KE4), the rmsd of Cα positions of monomer 2 of the acyl complex is 0.15 Å.

One unusual feature within the covalent adduct of WT AmpC with cephalothin is that the O9 carbonyl oxygen of cephalothin is not bound in the electrophilic or oxyanion hole but is twisted about the Oγ-C8 bond so that the O9 oxygen is displaced approximately 1.5 Å from its expected location (Figure 3B). The O9 oxygen now interacts with Wat402, the deacylating water [12, 14, 16]. Because of the opening of the β-lactam ring, the dihydrothiazine ring of the acyl complex is free to rotate about the C6-C7 bond, like the product. Indeed, the carboxylate of the acyl ligand has rotated 66° from its initial position in the substrate, resulting in a displacement of the C4′ carbon of the carboxylate of 5.5 Å. In this position, the carboxylate picks up an interaction with Asn343; it has lost the interactions with Tyr150 and Thr316 observed in the precovalent substrate complex (Table 2). The rotation of the six-membered dihydrothiazine ring opens up that region of the active site of monomer 2, which then binds Wat402 and Wat403 [12, 16]. On the other side of the molecule, the R1 side chain has been displaced by about 0.7 Å relative to the substrate, most likely due to the repositioning of the O9 oxygen. Nevertheless, the R1 amide of cephalothin is still recognized by Gln120, Asn152, and the main chain oxygen of Ala318. The thiophene ring π stacks with Tyr221, much as in the precovalent substrate complex. The conforma-

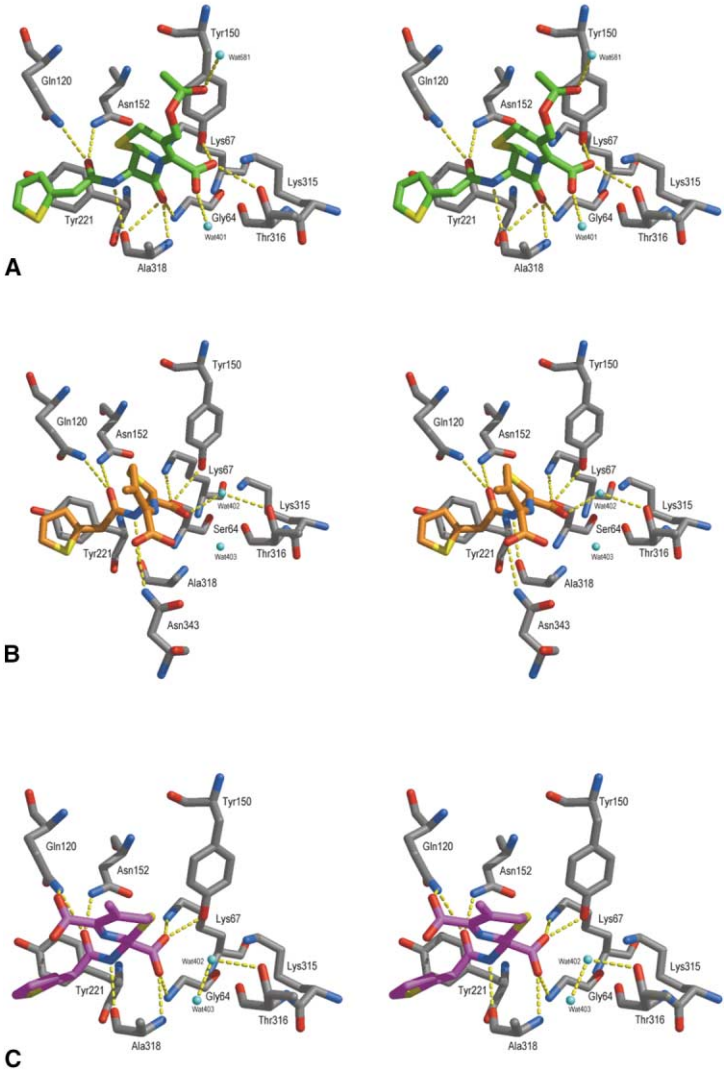

Figure 3. Stereoviews of Key Interactions Observed within Each Complexed Structure

(A) S64G/cephalothin enzyme-substrate complex.

(B) WT/cephalothin acyl complex.

(C) S64G/cephalothin enzyme-product complex.

Atoms are colored as in Figure 2, except that the carbon atoms of the substrate are green, the acyl ligand is orange, and the product is magenta, for clarity. Dashed yellow lines indicate interactions within hydrogen bonding distance; interaction distances are given in Table 2. Hydrogen bonds between protein residues are not shown. Figures 3 and 4 were generated using MidasPlus [53].

tion of the entire R1 group (Figure 1B) is quite similar to that observed in the precovalent substrate-enzyme complex, whereas the conformation of the dihydrothiazine ring is intermediate, between that of the substrate and the product (Figure 4B).

Discussion

To hydrolyze β-lactams, serine β-lactamases must recognize their substrate, form an acyl-adduct, and finally produce and expel the hydrolyzed product. Key aspects of how these perfect enzymes [20, 21] recognize substrate, activating it for hydrolytic attack, and how they bind substrate selectively over the product, avoiding measurable product inhibition, emerge from the precovalent substrate, acyl-intermediate, and postcovalent product complexes described here.

A Possible Role of Substrate in Activation of AmpC for Catalysis

In the precovalent encounter complex, the substrate cephalothin makes several interactions that are familiar from acyl-enzyme structures; several unexpected interactions are also observed. The interactions between the enzyme and the R1 side chain of cephalothin and between the electrophilic [11] or oxyanion [29] hole residues of the enzyme closely resemble those seen in earlier structures. Less expected is the placement of the characteristic C4′ carboxylate (Figure 1B) to accept a hydrogen bond from Tyr150 (Figure 3A), a residue previously implicated as the catalytic base [8, 9]. Several investigators have suggested that the substrate carboxylate could have a role in activating the β-lactamase for catalysis in both class A [31] and class C enzymes [32–34]. The structure of the precovalent substrate complex suggests that the C4′ carboxylate may activate Tyr150, which in turn may abstract a proton from Ser64 (which is 2.9 Å from the Tyr150 in the WT apo structure), either directly or via Lys67, to activate the serine for hydrolytic attack. This substrate-assisted mechanism may also be allowed by other hydrogen bond-accepting groups at this C4′ position [35].

In the covalent adduct between cephalothin and WT AmpC (Figure 3B), the C4′ carboxylate has moved by

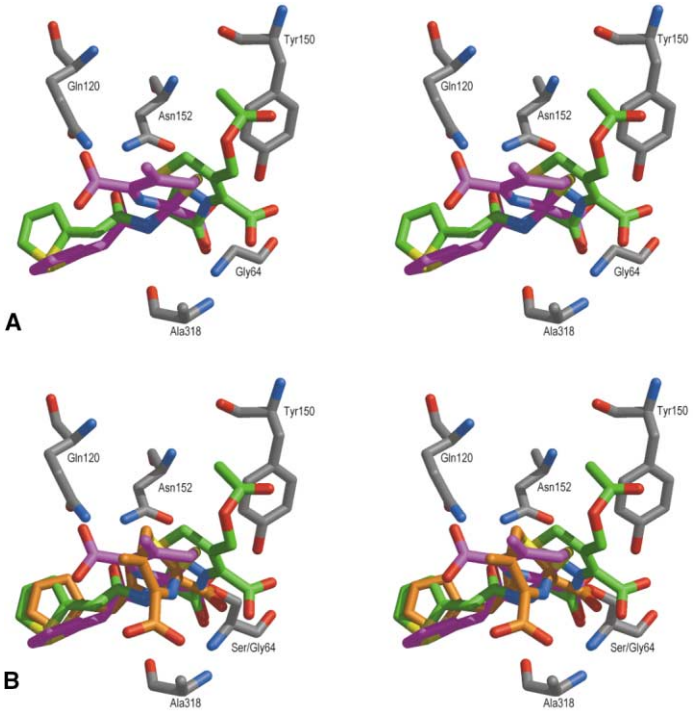

Figure 4. Stereoviews of the Superimposed Complexes of Cephalothin with AmpC Showing the Progression of the Reaction

The protein residues displayed are those of monomer 2 of the S64G/cephalothin complexed structure, which are almost identical with those of the other complexed structures. In (A), the complexes of S64G with the substrate (carbon atoms, green) and product (carbon atoms, magenta) are superimposed, showing the full extent of the rotation of the six-membered ring. In (B), the substrate (carbon atoms, green), acyl-intermediate (carbon atoms, orange), and product (carbon atoms, magenta) are overlaid, showing the progression of the reaction.

5.5 Å from its initial position in the precovalent substrate-enzyme complex, adopting a position similar to that seen in the complex between the substrate loracarbef and the deacylation-deficient mutant AmpC Y150E/Q120L [12]. This conformation opens the position for the presumptive hydrolytic water Wat402 [12–14, 16], which, in the precovalent substrate-enzyme complex, had been occupied by this carboxylate. Absent from the substrate-enzyme complex, Wat402 has reappeared in the acyl-enzyme complex, hydrogen bonding with Thr316 and within 3.4 Å of Tyr150, poised for hydrolytic attack on the acyl-intermediate. This suggests that class C β-lactamases, like class D β-lactamases [36, 37], use a symmetrical mechanism for hydrolysis. In the preacylation encounter complex, the C4′ carboxylate of the substrate appears to accept a hydrogen bond from Tyr150, which in turn accepts a hydrogen bond from Ser64, activating the serine for nucleophilic attack on the β-lactam bond of the substrate (Figure 5). On deacylation, Wat402 donates a hydrogen bond back to Tyr150, which in turn can donate a hydrogen bond to the Ser64Oγ, activating the serine to be a leaving group for deacylation.

Following deacylation, in the final, postcovalent product-enzyme complex (Figure 3C), the C4′ carboxylate has moved still further, to 7.3 Å from its original position in the precovalent substrate-enzyme complex (Figures 4A and 4B). Indeed, in the product complex with S64G, the entire dihydrothiazine ring has rotated by 109° around the C6-C7 bond so that it is almost "upside down" compared to the fused ring position in the precovalent complex (Figure 4A). This rotation probably reflects electrostatic repulsion between the C4′ carboxylate and the newly formed carboxylate at C8. If the dihydrothiazine ring did not rotate, this newly formed carboxylate would be within 3.3 Å of the C4′ carboxylate. In its final position, the C4′ carboxylate forces a rotation of the thiophene ring of the R1 side chain, disrupting the π-stacking interaction between it and Tyr221. The altered conformation of the product and the resultant loss of interactions of both the C4′ carboxylate and the thiophene ring may account for the low binding affinity of product to AmpC. Product inhibition, which can be significant in many enzymes, has not been reported for serine β-lactamases. This appears to owe to inherent strain in the product itself; the two carboxylates require a significant conformational change, which then disrupts binding of other regions of the ligand to the active site.

The Role of the R2 Leaving Group

Within the substrate-enzyme complex, the placement of the R2 side chain (Figure 1B) is interesting because it seems so little involved in the complex. This side chain is displaced through an electronic rearrangement after the β-lactam ring has been opened in the acyl-adduct, leaving a single exocyclic methylene group at C3′. It is this form of cephalothin, where the R2 side chain has been displaced, that is captured in the acyl-enzyme and product complexes (Figures 3B and 3C; Table 2) described here and that has been seen in all previous cephalosporin complexes with β-lactamases [12, 13, 38] and penicillin binding proteins [39, 40]. Because the β-lactam ring has not opened in the encounter complex (Figure 3A), this R2 side chain is still present. Investigators have made many substitutions at this site and have found that both bulky groups, such as the 2,4-dinitrostyryl side chain in nitrocefin, and small groups, such as the chlorine in cefaclor, are tolerated. Medicinal chemists have used this tolerance to place very large group groups at this position as a tool for drug delivery [41,

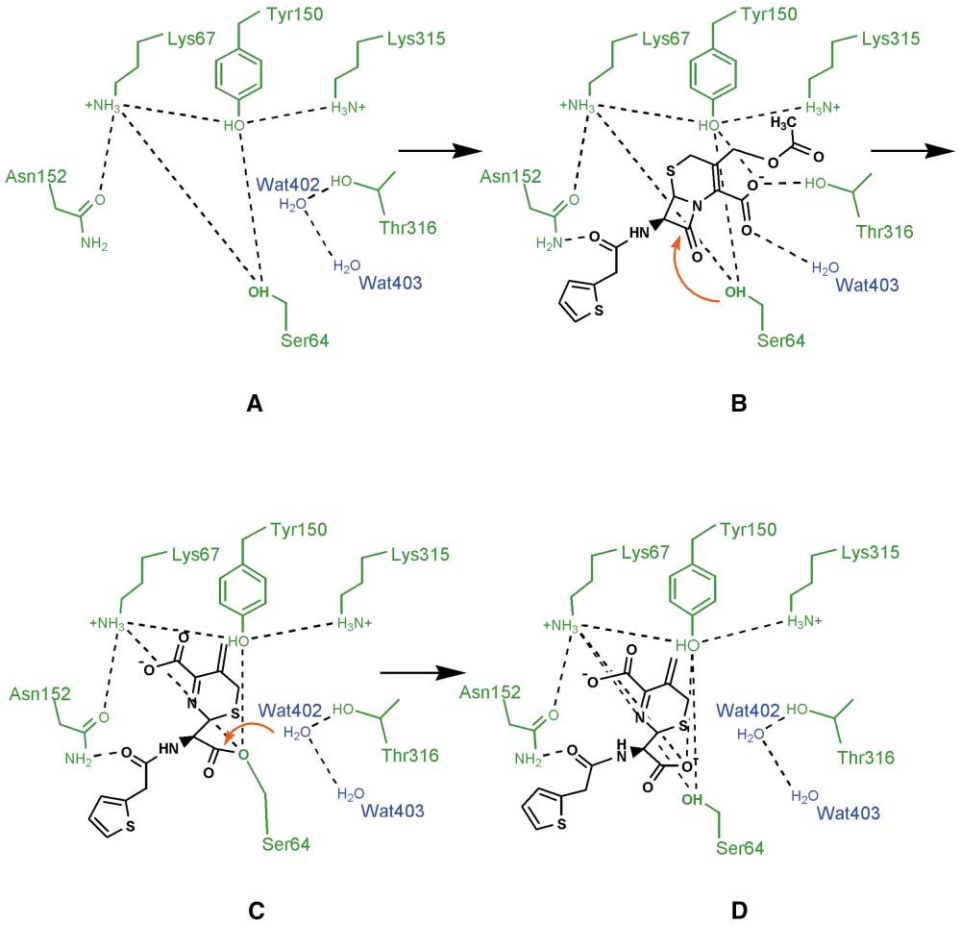

Figure 5. Cartoon of Several Key Interactions in the Proposed Mechanism of AmpC β-Lactamase

In (A), the apo enzyme is shown with Wat402 and Wat403 bound. In (B), the substrate is shown bound in the active site. Wat402, the putative deacylating water, is displaced by the C4′ carboxylate, which activates Tyr150, which may in turn activate Ser64 to attack the C8 carbonyl carbon of the β-lactam ring. In (C), the acyl-adduct is shown. Wat402 resumes its position, and it is activated for attack at the C8 carbonyl carbon. Finally, in (D), the product is shown bound to the active site; Wat402 and Wat403 are present. Protein atoms, green; ligand atoms, black; waters, blue; dotted lines indicate selected hydrogen bonds, and red arrows indicate the direction of attack.

42] and as immunomodulators [43]. As far as the class C β-lactamases are concerned, the structure of the precovalent substrate-enzyme complex explains this tolerance—the R2 side chain makes few interactions with the enzyme, instead pointing out toward solvent. No obvious restrictions on the size of this side chain appear from the substrate-enzyme complex.

Realistic Views of the Intermediates?

It is appropriate to consider certain caveats when interpreting these structures. First, how much does the residue substitution at Ser64 affect the binding of the ligand? The truncation of this side chain clearly allows both the substrate and product to come closer to the enzyme in the region of residue 64 than would be possible in the WT form. Overlaying the substrate/S64G structure with the WT apo structure, the catalytic Ser64Oγ would be 1.9 Å from the C8 carbonyl carbon of the lactam ring, which is closer to a covalent distance than a van der Waals distance. Nevertheless, even the proximal portions of both the substrate (O9 lactam oxygen) and the product (O9A and O9B oxygens of the carboxylate) would be able to make similar contacts in the WT enzyme. The more distal portions of the molecule, for instance, the amide of the R1 side chain, overlay almost exactly with those of the acyl complexes previously determined [12], suggesting a realistic placement of both substrate and product.

Second, why have we been able to capture the substrate in one monomer and the product of the reaction in the other monomer of the S64G crystal? Class C β-lactamases are active as monomers; however, AmpC crystallizes with two monomers in each asymmetric unit, and each monomer adopts a slightly different conformation. In monomer 1, the region of residues 280–295 usually is relatively disordered; residues 289–295 adopt a loop conformation, making the active site more open in the region around the substrate's R2 side chain. In monomer 2, these residues (289–295) fold into two turns of a helix, causing Leu293 to move 4 Å (Cα to Cα) to 7 Å (Cγ to Cγ) into the active site, closing off the region that was occupied by the distal portion of the R2 leaving

group. Substrate binds to the more open conformation of monomer 1, and product binds to the more closed conformation of monomer 2. We note that when transition-state analogs are cocrystallized with AmpC, both monomers adopt closed conformations [16, 17]. Similarly, in soaking experiments with β-lactams, the acyl-enzyme complex is usually more ordered in monomer 2, which adopts the more closed conformation [12, 13]. There may be two functionally important conformations of this region in class C β-lactamases: a more open conformation that binds to substrate and a more closed conformation that occurs as the reaction proceeds. Except for this one region, we note that AmpC itself undergoes little overall conformational change as the reaction proceeds from the apo enzyme to substrate, acyl, deacylation transition-state analog, and product complexes.

Finally, how have we been able to capture the WT enzyme with an excellent substrate, like cephalothin, in an acyl-adduct? We believe that the alteration in the position of the O9 oxygen, which is no longer in the electrophilic or oxyanion hole and hence is not competent for deacylation, was crucial to the capture of this complex. The idea that the ester of the acyl-adduct in β-lactamases may adopt alternate conformations has been previously suggested based on FTIR evidence [44, 45]. Indeed, these authors have suggested that the lack of evidence for such alternate conformations in X-ray crystal structures points out the inability of crystallography to reliably capture higher-energy states. This structure confirms the possibility of this rotational movement within the acyl-adduct crystallographically. As far as the interpretation of the acyl-adduct is concerned, the movement of the O9 oxygen does not appear to alter the rest of the structure significantly; the entire molecule, save the O9, overlays well with the structure of loracarbef determined in complex with a deacylation-deficient mutant enzyme [12]. This leads us to believe that the interactions observed outside the region around the O9 oxygen may be used to understand the mechanism of AmpC.

Conclusions

A proficient enzyme must recognize its substrate, activating it for catalysis, and must selectively bind the substrate over the product to avoid product inhibition. Exactly how this is done remains an area of active inquiry for many hydrolases. For the class C β-lactamases, the following model may now be proposed (Figure 5). First, AmpC binds its substrate; there is no discernible conformational change on complex formation. Once bound, the substrate is oriented using a network of hydrogen bonds and nonpolar interactions that stretch across the entire molecule, stopping only at the displaceable R2 side chain (Figure 3A). A hydrogen bond between the C4′ carboxylate of the substrate itself and Tyr150 may activate the latter, the presumed catalytic base [6, 8], to transiently accept a proton from the nucleophilic Ser64, priming it for attack on the substrate. An intermediary role for Lys67 in this transfer cannot be ruled out at this time. After the attack of Ser64 and the formation of the acyl-adduct, this C4′ carboxylate swings into a new position, 5.5 Å away from where it was in the encounter complex. This displacement allows the deacylating water to bind to its staging site, where it is activated by Thr316 and possibly Tyr150 (see also [12–14, 16]). As previously described [12, 13], attack by this water leads to a tetrahedral adduct, where Tyr150 may participate with the dihydrothiazine nitrogen of the substrate itself [46] to stabilize this high-energy intermediate. Collapse of this intermediate leads to formation of product, and the C4′ carboxylate rotates even further away from its original position in the precovalent substrate-enzyme complex. The driving force for this rotation may be the internal electrostatic strain between the C4′ carboxylate and the newly formed carboxylate at C8. Its consequence is that key favorable hydrogen bonds are broken. This, combined with the difficulty in desolvating a dianionic species, results in the low affinity of product for AmpC relative to substrate. β-lactams are highly functionalized molecules, and AmpC appears to take advantage of that functionality not only as handles for recognition, as in classic enzyme-ligand recognition, but also to actually activate the enzyme at several stages in the mechanism.

Biological Implications

Serine hydrolases, which include proteases and β-lactamases, are a widely studied class of enzymes involved in many diseases. β-lactamases are the leading cause of bacterial resistance to β-lactam antibiotics, like penicillins and cephalosporins. Despite the impact of these enzymes on public health, little is known about the structural basis of substrate recognition and selective binding of substrate over the hydrolyzed product of the reaction. Understanding each step of the hydrolysis would help to explain the observed differences in activity between different enzymes and the importance of specific moieties of their substrates. To better understand these features, the crystal structures of AmpC β-lactamase in complex with the substrate, acyl, and product forms of a good substrate have been determined. We observe that the ligand itself undergoes a significant conformational change as the reaction progresses. These structures suggest that conserved portions of the ligand are crucial for activating the enzyme at each stage of the reaction. This observation may provide a way to design new hydrolase inhibitors; if the enzymes depend on the ligand for activation, alterations in the ligand that eliminate these interactions may act as inhibitors. These snapshots along the reaction pathway of β-lactam hydrolysis thus not only provide insight into the mechanism of serine hydrolases but may also help to design new β-lactam antibiotics that can resist hydrolysis by β-lactamases.

Experimental Procedures

Enzyme Preparation

The mutant AmpC S64G was made using the overlap extension polymerase chain reaction (PCR) [47]. The mutagenesis of the ampC gene was performed in the pOGO295 plasmid [11]. Following PCR mutagenesis, the mutant gene was cut using XbaI and BamHI (New England Biolabs, Beverly, MA) to create sticky ends and ligated back into the plasmid, which had been similarly cut. The mutant

plasmid was then transformed into *Escherichia coli* JM109 using electroporation.

Both AmpC S64G and WT were expressed as previously described [11, 48]. The WT enzyme was purified from an *m*-aminophenylboronic acid affinity column [11], and the S64G enzyme was purified from an S-Sepharose ion exchange column [12].

Crystal Growth

Crystals of AmpC WT and S64G were grown by vapor diffusion in 6 μl hanging drops over a solution of 1.7 M potassium phosphate (pH 8.7) after microseeding with wild-type enzyme [11]. Crystals were grown at 23°C and appeared within 5–7 days. Crystals of apo S64G and of WT AmpC were harvested using nylon loops and each placed in an individual 6 μl drop of saturated cephalothin and 1.7 M potassium phosphate (pH 8.7), and then more cephalothin powder was sprinkled on the drop. Both crystals were soaked in cephalothin drops suspended over a 1 ml well of crystallizing buffer; the S64G crystal was soaked for 3 hr, and the WT crystal was soaked for 15 min and then transferred to a fresh drop for another 15 min. Following the cephalothin soaks, both the S64G and WT crystals were immersed in a cryoprotectant solution of saturated cephalothin, 25% sucrose, and 1.7 M potassium phosphate (pH 8.7) for approximately 20 s and then flash cooled in liquid nitrogen.

Data Collection, Processing, and Refinement

X-ray diffraction data were measured at the DND-CAT beamline 5IDB at the Advanced Photon Source at Argonne National Laboratory at 100K using a 162 mm Mar CCD detector. The reflections were indexed, integrated, and scaled using the HKL package [49] (Table 1). AmpC crystallizes in the C2 space group, with two AmpC molecules per asymmetric unit.

For S64G/cephalothin, an initial model, an AmpC/boronic acid complexed structure (Protein Data Bank entry 1C3B) [16], with inhibitor and solvent atoms removed and glycine substituted for Ser64, was positioned by rigid body refinement. For WT/cephalothin, an initial model, a different AmpC/boronic acid complexed structure (Protein Data Bank entry 1FSY) [17], with inhibitor and solvent atoms removed, was also positioned by rigid body refinement. The models were then refined using simulated annealing, positional minimization, and individual B factor refinement with the maximum likelihood target, a bulk solvent correction, and a 2 σ cutoff with CNS [50]. σ_A-weighted electron density maps were also calculated with CNS [50]. The cephalothin molecules were built into the observed difference density in each active site. Manual rebuilding of the model and placement of water molecules using the program O [51] were then alternated with rounds of positional and B factor refinement with CNS using all data from 20 to 1.53 Å.

For S64G/cephalothin, occupancies of the ligands were determined based on optimization of difference density and by comparison of the refined thermal factors. Cephalothin in monomer 1 was modeled as the substrate closed ring form and refined with an occupancy of 0.65; the average thermal factor for the substrate was 49.3 Å^2, ranging from 34.5 Å^2 to 64.8 Å^2. Cephalothin in monomer 2 was modeled as the product hydrolyzed form and refined with an occupancy of 0.9; the average thermal factor for the product was 42.5 Å^2, ranging from 30.0 Å^2 to 50.8 Å^2. In addition to these two active site ligands, two phosphate ions were modeled in the S64G/cephalothin structure; one phosphate overlaps the substrate in the active site of monomer 1, representing a portion of unit cells that lacked the ligand, and was modeled with an occupancy of 0.35. A second phosphate is found at a crystal contact. In addition, Lys164 of monomer 1 was observed to have a covalently bound cephalothin molecule in two conformations; each was modeled at half occupancy. We do not believe that this is a relevant binding site because it occurs at a crystal contact and is not seen in monomer 2, where there is no similar interaction with a symmetry mate. For the S64G/cephalothin complex, each monomer contains 358 residues. Due to poor electron density in the region 280–295 of monomer 1, some residues were modeled as alanine.

For WT/cephalothin, occupancy of the ligand was based on a comparison of refined thermal factors of the ligand with those of the covalently bound Ser64. Cephalothin in monomer 2 was modeled as the covalent adduct with an occupancy of 0.8; the average thermal factor was 50.5 Å^2, ranging from 43.6 Å^2 to 57.6 Å^2. No ligand was modeled in monomer 1. For the WT/cephalothin complex, monomer 2 contains 358 residues; monomer 1 contains only 354 residues due to poor electron density in the region 280–295; residues 287 and 290–292 were excluded from the model. Other residues in this region were modeled as alanine due to poor side chain density.

The coordinates for the AmpC S64G and WT structures in complex with cephalothin have been deposited in the Protein Data Bank with accession codes 1KVL and 1KVM, respectively.

Acknowledgments

This work was supported by NIH GM63815 (to B.K.S.). B.M.B. was partly supported by NIH training grant GM08382 (Robert MacDonald, PI). I.T. is a Howard Hughes Medical Institute Medical Student Research Training Fellow. We thank Rachel Powers, Xiaojun Wang, and Susan McGovern for reading this manuscript and Rachel Powers for assistance with crystallographic methods. Crystallography data were collected at the DuPont-Northwestern-Dow Collaborative Access Team at the APS, which is supported by E.I. DuPont, de-Nemours & Co., the Dow Chemical Company, the NSF, and the State of Illinois.

References

1. Neu, H.C. (1992). The crisis in antibiotic resistance. Science *257*, 1064–1073.
2. Davies, J. (1994). Inactivation of antibiotics and the dissemination of resistance genes. Science *264*, 375–382.
3. Bush, K., Jacoby, G.A., and Medeiros, A.A. (1995). A functional classification scheme for beta-lactamases and its correlation with molecular structure. Antimicrob. Agents Chemother. *39*, 1211–1233.
4. Tsukamoto, K., Tachibana, K., Yamazaki, N., Ishii, Y., Ujiie, K., Nishida, N., and Sawai, T. (1990). Role of lysine-67 in the active site of class C beta-lactamase from Citrobacter freundii GN346. Eur. J. Biochem. *188*, 15–22.
5. Monnaie, D., Dubus, A., and Frere, J.M. (1994). The role of lysine-67 in a class C beta-lactamase is mainly electrostatic. Biochem. J. *302*, 1–4.
6. Dubus, A., Normark, S., Kania, M., and Page, M.G. (1994). The role of tyrosine 150 in catalysis of beta-lactam hydrolysis by AmpC beta-lactamase from Escherichia coli investigated by site-directed mutagenesis. Biochemistry *33*, 8577–8586.
7. Dubus, A., Normark, S., Kania, M., and Page, M.G. (1995). Role of asparagine 152 in catalysis of beta-lactam hydrolysis by Escherichia coli AmpC beta-lactamase studied by site-directed mutagenesis. Biochemistry *34*, 7757–7764.
8. Dubus, A., Ledent, P., Lamotte-Brasseur, J., and Frere, J.M. (1996). The roles of residues Tyr150, Glu272, and His314 in class C beta-lactamases. Proteins *25*, 473–485.
9. Oefner, C., D'Arcy, A., Daly, J.J., Gubernator, K., Charnas, R.L., Heinze, I., Hubschwerlen, C., and Winkler, F.K. (1990). Refined crystal structure of beta-lactamase from Citrobacter freundii indicates a mechanism for beta-lactam hydrolysis. Nature *343*, 284–288.
10. Lobkovsky, E., Moews, P.C., Liu, H., Zhao, H., Frere, J.M., and Knox, J.R. (1993). Evolution of an enzyme activity: crystallographic structure at 2-Å resolution of cephalosporinase from the ampC gene of Enterobacter cloacae P99 and comparison with a class A penicillinase. Proc. Natl. Acad. Sci. USA *90*, 11257–11261.
11. Usher, K.C., Blaszczak, L.C., Weston, G.S., Shoichet, B.K., and Remington, S.J. (1998). Three-dimensional structure of AmpC beta-lactamase from Escherichia coli bound to a transition-state analogue: possible implications for the oxyanion hypothesis and for inhibitor design. Biochemistry *37*, 16082–16092.
12. Patera, A., Blaszczak, L.C., and Shoichet, B.K. (2000). Crystal structures of substrate and inhibitor complexes with AmpC beta-lactamase: possible implications for substrate-assisted catalysis. J. Am. Chem. Soc. *122*, 10504–10512.
13. Powers, R.A., Caselli, E., Focia, P.J., Prati, F., and Shoichet, B.K. (2001). Structures of ceftazidime and its transition-state

analogue in complex with AmpC beta-lactamase: implications for resistance mutations and inhibitor design. Biochemistry *40*, 9207–9214.

14. Crichlow, G.V., Nukaga, M., Doppalapudi, V.R., Buynak, J.D., and Knox, J.R. (2001). Inhibition of class C beta-lactamases: structure of a reaction intermediate with a cephem sulfone. Biochemistry *40*, 6233–6239.
15. Lobkovsky, E., Billings, E.M., Moews, P.C., Rahil, J., Pratt, R.F., and Knox, J.R. (1994). Crystallographic structure of a phosphonate derivative of the Enterobacter cloacae P99 cephalosporinase: mechanistic interpretation of a beta-lactamase transition-state analog. Biochemistry *33*, 6762–6772.
16. Powers, R.A., Blazquez, J., Weston, G.S., Morosini, M.I., Baquero, F., and Shoichet, B.K. (1999). The complexed structure and antimicrobial activity of a non-beta-lactam inhibitor of AmpC beta-lactamase. Protein Sci. *8*, 2330–2337.
17. Caselli, E., Powers, R.A., Blasczcak, L.C., Wu, C.Y., Prati, F., and Shoichet, B.K. (2001). Energetic, structural, and antimicrobial analyses of beta-lactam side chain recognition by beta-lactamases. Chem. Biol. *8*, 17–31.
18. Galleni, M., and Frere, J.M. (1988). A survey of the kinetic parameters of class C beta-lactamases. Penicillins. Biochem. J. *255*, 119–122.
19. Galleni, M., Amicosante, G., and Frere, J.M. (1988). A survey of the kinetic parameters of class C beta-lactamases. Cephalosporins and other beta-lactam compounds. Biochem. J. *255*, 123–129.
20. Christensen, H., Martin, M.T., and Waley, S.G. (1990). Beta-lactamases as fully efficient enzymes. Determination of all the rate constants in the acyl-enzyme mechanism. Biochem. J. *266*, 853–861.
21. Bulychev, A., and Mobashery, S. (1999). Class C beta-lactamases operate at the diffusion limit for turnover of their preferred cephalosporin substrates. Antimicrob. Agents Chemother. *43*, 1743–1746.
22. Harel, M., Su, C.T., Frolow, F., Silman, I., and Sussman, J.L. (1991). Gamma-chymotrypsin is a complex of alpha-chymotrypsin with its own autolysis products. Biochemistry *30*, 5217–5225.
23. Rose, R.B., Craik, C.S., Douglas, N.L., and Stroud, R.M. (1996). Three-dimensional structures of HIV-1 and SIV protease product complexes. Biochemistry *35*, 12933–12944.
24. Martin, P.D., Malkowski, M.G., DiMaio, J., Konishi, Y., Ni, F., and Edwards, B.F. (1996). Bovine thrombin complexed with an uncleavable analog of residues 7–19 of fibrinogen A alpha: geometry of the catalytic triad and interactions of the P1′, P2′, and P3′ substrate residues. Biochemistry *35*, 13030–13039.
25. Sadasivan, C., and Yee, V.C. (2000). Interaction of the factor XIII activation peptide with alpha-thrombin. Crystal structure of its enzyme-substrate analog complex. J. Biol. Chem. *275*, 36942–36948.
26. Silvaggi, N.R., McDonough, M.A., Brinsmade, S.R., Knox, J.R., and Kelly, J.A. (2001). Observation of Michaelis and product complexes between a peptide substrate and D-Ala-D-Ala-peptidase. In American Crystallographic Association, Inc. 2001 Annual Meeting, Los Angeles (Buffalo, NY: American Crystallographic Association), p.139
27. Hrmova, M., Varghese, J.N., De Gori, R., Smith, B.J., Driguez, H., and Fincher, G.B. (2001). Catalytic mechanisms and reaction intermediates along the hydrolytic pathway of a plant beta-D-glucan glucohydrolase. Structure *9*, 1005–1016.
28. Laskowski, R.A., MacArthur, M.W., Moss, D.S., and Thornton, J.M. (1993). PROCHECK: a program to check the stereochemical quality of protein structures. J. Appl. Crystallogr. *26*, 283–291.
29. Murphy, B.P., and Pratt, R.F. (1988). Evidence for an oxyanion hole in serine beta-lactamases and DD- peptidases. Biochem. J. *256*, 669–672.
30. Kelly, J.A., Knox, J.R., and Zhao, H.C. (1989). Studying enzyme-beta-lactam interactions using x-ray diffraction. J. Mol. Graph. *7*, 87–92.
31. Atanasov, B.P., Mustafi, D., and Makinen, M.W. (2000). Protonation of the beta-lactam nitrogen is the trigger event in the catalytic action of class A beta-lactamases. Proc. Natl. Acad. Sci. USA *97*, 3160–3165.
32. Thornewell, S.J., and Waley, S.G. (1992). Site-directed mutagenesis and substrate-induced inactivation of beta-lactamase I. Biochem. J. *288*, 1045–1051.
33. Ishiguro, M., and Imajo, S. (1996). Modeling study on a hydrolytic mechanism of class A beta-lactamases. J. Med. Chem. *39*, 2207–2218.
34. Bulychev, A., Massova, I., Miyashita, K., and Mobashery, S. (1997). Nuances of mechanisms and their implications for evolution of the versatile beta-lactamase activity: from biosynthetic enzymes to drug resistance factors. J. Am. Chem. Soc. *119*, 7619–7625.
35. Varetto, L., De Meester, F., Monnaie, D., Marchand-Brynaert, J., Dive, G., Jacob, F., and Frere, J.M. (1991). The importance of the negative charge of beta-lactam compounds in the interactions with active-site serine DD-peptidases and beta-lactamases. Biochem. J. *278*, 801–807.
36. Massova, I., and Mobashery, S. (1998). Kinship and diversification of bacterial penicillin-binding proteins and beta-lactamases. Antimicrob. Agents Chemother. *42*, 1–17.
37. Golemi, D., Maveyraud, L., Ishiwata, A., Tranier, S., Miyashita, K., Nagase, T., Massova, I., Mourey, L., Samama, J.P., and Mobashery, S. (2000). 6-(hydroxyalkyl)penicillanates as probes for mechanisms of beta- lactamases. J. Antibiot. (Tokyo) *53*, 1022–1027.
38. Chen, C.C., and Herzberg, O. (2001). Structures of the acyl-enzyme complexes of the Staphylococcus aureus beta-lactamase mutant Glu166Asp:Asn170Gln with benzylpenicillin and cephaloridine. Biochemistry *40*, 2351–2358.
39. Kuzin, A.P., Liu, H., Kelly, J.A., and Knox, J.R. (1995). Binding of cephalothin and cefotaxime to D-ala-D-ala-peptidase reveals a functional basis of a natural mutation in a low-affinity penicillin-binding protein and in extended-spectrum beta-lactamases. Biochemistry *34*, 9532–9540.
40. Gordon, E., Mouz, N., Duee, E., and Dideberg, O. (2000). The crystal structure of the penicillin-binding protein 2x from Streptococcus pneumoniae and its acyl-enzyme form: implication in drug resistance. J. Mol. Biol. *299*, 477–485.
41. Mobashery, S., and Johnston, M. (1986). Reactions of Escherichia coli TEM beta-lactamase with cephalothin and with C10-dipeptidyl cephalosporin esters. J. Biol. Chem. *261*, 7879–7887.
42. Ishikawa, T., Nakayama, Y., Tomimoto, M., Niwa, S.I., Kamiyama, K., Hashiguchi, S., Iizawa, Y., Okonogi, K., and Miyake, A. (2001). Studies on anti-MRSA parenteral cephalosporins. IV. A novel water-soluble N-phosphono type prodrug for parental administration. J. Antibiot. (Tokyo) *54*, 364–374.
43. Labro, M.T., and el Benna, J. (1990). Comparison of cefodizime with various cephalosporins for their indirect effect on the human neutrophil oxidative burst in vitro. J. Antimicrob. Chemother. *26* (*Suppl C*), 49–57.
44. Wilkinson, A.S., Ward, S., Kania, M., Page, M.G., and Wharton, C.W. (1999). Multiple conformations of the acylenzyme formed in the hydrolysis of methicillin by Citrobacter freundii beta-lactamase: a time-resolved FTIR spectroscopic study. Biochemistry *38*, 3851–3856.
45. Hokenson, M.J., Cope, G.A., Lewis, E.R., Oberg, K.A., and Fink, A.L. (2000). Enzyme-induced strain/distortion in the ground-state ES complex in beta-lactamase catalysis revealed by FTIR. Biochemistry *39*, 6538–6545.
46. Maveyraud, L., Mourey, L., Kotra, L.P., Pedelacq, J., Guillet, V., Mobashery, S., and Samama, J. (1998). Structural basis for clinical longevity of carbapenem antibiotics in the face of challenge by the common class A beta-lactamases from the antibiotic-resistant bacteria. J. Am. Chem. Soc. *120*, 9748–9752.
47. Ho, S.N., Hunt, H.D., Horton, R.M., Pullen, J.K., and Pease, L.R. (1989). Site-directed mutagenesis by overlap extension using the polymerase chain reaction. Gene *77*, 51–59.
48. Trehan, I., Beadle, B.M., and Shoichet, B.K. (2001). Inhibition of AmpC beta-lactamase through a destabilizing interaction in the active site. Biochemistry *40*, 7992–7999.
49. Otwinowski, Z., and Minor, W. (1997). Processing of X-ray diffraction data collected in oscillation mode. Methods Enzymol. *276*, 307–326.
50. Brunger, A.T., Adams, P.D., Clore, G.M., DeLano, W.L., Gros, P., Grosse-Kunstleve, R.W., Jiang, J.S., Kuszewski, J., Nilges,

M., Pannu, N.S., et al. (1998). Crystallography and NMR system: a new software suite for macromolecular structure determination. Acta Crystallogr. D *54*, 905–921.

51. Jones, T.A., Zou, J.Y., Cowan, S.W., and Kjeldgaard, M. (1991). Improved methods for building protein models in electron density maps and the location of errors in these models. Acta Crystallogr. A *47*, 110–119.
52. Evans, S.V. (1993). SETOR: hardware-lighted three-dimensional solid model representations of macromolecules. J. Mol. Graph. *11*, 134–138, 127–128.
53. Ferrin, T.E., Huang, C.C., Jarvis, L.E., and Langridge, R. (1988). The MIDAS display system. J. Mol. Graph. *6*, 13–27.

Accession Numbers

The coordinates for the AmpC S64G and WT structures in complex with cephalothin have been deposited in the Protein Data Bank with accession codes 1KVL and 1KVM, respectively.